Multidetector-row Computed Tomographic Evaluation of the Fine Vascular Structures

Kei Takase, Li Li, and Shoki Takahashi*

* Professor
Department of Radiology, Graduate School of Medicine
E-mail: ktakase@rad.med.tohoku.ac.jp, t-shoki@rad.med.tohoku.ac.jp

Abstract

We analyzed fine vascular structures of normal subject in 2007 in g-COE program. This year, we applied our technique to visualize fine vascular structures to patients with primary aldosteronism and aortic aneurysm to evaluate clinical utility of fine vessel visualization. Our project contains the analysis of the adrenal vein and the artery of Adamkiewicz, both of which have been thought to be difficult to visualize.

Visualization of the adrenal vein

Selective adrenal venous sampling, which is indispensable for the differential diagnosis of primary aldosteronism, is a technically difficult procedure. We evaluated the accuracy of multidetector-row computed tomography (MDCT) in the detection of right adrenal vein. MDCT evaluation about the location of the orifice, transverse and vertical direction, and relationship to other fine retroperitoneal veins using 64-detector row scanner in 60 patients with primary aldosteronism were compared to angiographic diagnosis during selective bilateral adrenal venous sampling. The right adrenal vein was detected by MDCT in all patients. Pre-angiographic MDCT information well coincided with angiographic findings enabling successful adrenal venous sampling.

Introduction

Primary aldosteronism is the most common form of secondary hypertension, and its prevalence in hypertensive populations is estimated at approximately 10% [1-8]. Unilateral aldosterone-producing adenoma and bilateral idiopathic hyperaldosteronism are the two most common subtypes of primary aldosteronism, and distinguishing between them is critical for treatment planning. Adrenalectomy in patients with a unilateral aldosterone-producing adenoma mitigates hypertension, while hypertension due to bilateral idiopathic hyperaldosteronism is treated medically. Adrenal venous sampling is an essential diagnostic step [5-8].A recent multicenter study revealed that 4.8 % of hypertension patients had aldosterone producing adenoma (APA) which is a curable form of primary aldosteronism [4]. MDCT and MRI, which are able to detect small adrenal adenoma, are not a reliable method in the differential diagnosis of primary aldosteronism [2-6] because aldosterone may be produced in the contrarateral side of the adrenal adenoma.

Selective adrenal venous sampling is difficult to perform because catheterization of the right adrenal vein (RAV) generally remains difficult with a success rate of approximately 70% [1-2], whereas catheterization of the left adrenal vein is a simple procedure. Right adrenal vein, generally 1-2mm in diameter, drains directly into inferior vena cava, which makes selective catheterization difficult, while left adrenal vein drains into left renal vein. [Fig. 1]

Multi-detector row CT (MDCT) could possibly guide adrenal venous sampling if it were capable of delineating the anatomy of the RAV [9]. We have reported a detailed analysis regarding visualizing the anatomy of the RAV with MDCT referring to the accurately the RAV could be evaluated on MDCT compared to adrenal venography and to evaluate the effectiveness of pre-angiographic visualization of the RAV in the management of primary aldosteronism.

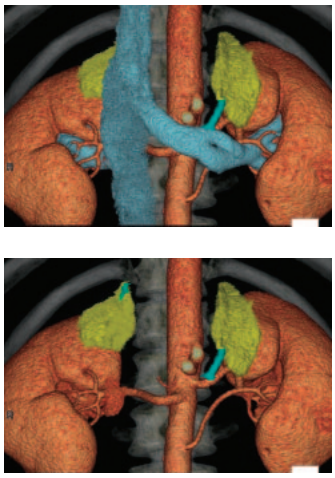

Fig. 1. Three dimensional reconstruction of the adrenal anatomy by MDCT images. Abdominal arterial structures and both kidneys are colored in orange, both adrenal grands in yellow, adrenal veins in blue, and other venous structures in light blue.

Materials and Methods

The institutional review board approved this study; informed consent was not required for this retrospective study.

Patients

We performed a retrospective analysis of CT images from 42 consecutive patients (20 men, 22 women; mean age, 55.3 years; range, 24–76 years) with a presumptive diagnosis of primary aldosteronism who underwent both contrast-enhanced MDCT of the upperabdomen and selective bilateral adrenal venous sampling between April 2007 and July 2007. Informed consent for contrast-enhanced CT and adrenal venous sampling had been obtained from all patients before the examinations.

CT examination

The CT scanner was an Aquilion 64-detector row helical CT scanner (Toshiba, Tokyo, Japan). Scans were obtained with the following parameters: 0.5 second per rotation, 0.5 mm collimation, and 25 mm/sec table increment (pitch, 55). Patients were requested to hold their breath for approximately 10 seconds during the scanning.

Before scanning was started, 100 mL of a contrast material containing 300 mg of iodine per milliliter (Iopamidol, Iopamiron; Schering, Berlin, Germany) was injected into an antecubital vein at a rate of 4.0 mL/sec. The scan delay was set by means of an automatic triggering system (SureStart; Toshiba). When the attenuation value at the level of the ascending aorta reached a preset threshold (an absolute attenuation value of 100 HU), Early-arterial-phase scanning automatically started. Late-arterial-phase scanning was begun immediately after the completion of the early arterial scanning. Venous phase scanning was begun 15 seconds after the completion of the late arterial scan followed by delayed-phase scanning 2 minutes after start of the injection. Transverse sections were reconstructed with a 0.5-mm section thickness at 0.5-mm intervals. For evaluating the RAV, the reconstruction field of view was set to the area around the aorta, inferior vena cava (IVC) and both kidneys.

CT interpretation

Images were interpreted using a stand-alone workstation (AQ station; Terarecon, Tokyo, Japan). We used a multiplanar reformation (MPR) display mode which enables simultaneous cine-mode observation of axial, coronal, and saggital MPR images to evaluate the RAV.

Points of evaluation

We evaluated the following points regarding the RAV partly based on the report of Matsuura et.al. [9]: whether the common trunk was formed before entering the IVC with accessory hepatic or other veins; the anatomy of the RAV including the location of the orifice, direction at the branching portion from the IVC,

1. Relationship of the RAV to an accessory hepatic vein

We examined whether a common trunk for the RAV and accessory hepatic or other veins was formed before entering the IVC. When the RAV directly entered the IVC but almost shared a common orifice with an accessory hepatic vein, or orifice of an accessory hepatic vein is nearly located to it was also recorded.

3. Location of the RAV orifice in relation to surrounding structures

The craniocaudal level of the RAV orifice was specified relative to vertebral bodies. The position of the orifice was also evaluated along the circumference of the IVC as an angle in the *x–y* plane (Fig. 1).

4. Direction of the RAV at the branching portion from the IVC

To evaluate the direction of the RAV at the branching portion from the IVC, two angles were measured: the first was the angle (X1) between the RAV and *x*-axis when the RAV was projected onto the *x–y* plane (Fig. 1), while the other was the craniocaudal angle (X2) between the RAV and z-axis when the RAV was projected onto the vertical plane that paralleled the RAV at the branching portion (Fig. 2).

Adrenal venous sampling

1. Method of venous sampling

In general, bilateral femoral vein puncture was performed to insert 7F-sheath. 6.5F-right and left adrenal venous catheters (Hanako, Tokyo, Japan) were used in most of the cases. First, the left adrenal venous catheter was inserted from the left femoral vein to select the left adrenal vein. The Rivage microcatheter was inserted into the peripheral part of the the left adrenal vein distal side to the inferior phrenic venous anastomosis to avoid dilution of the blood sample. Then the right adrenal venous catheter was inserted from the right adrenal vein. CT evaluation about the location of the right adrenal vein, such as craniocaudal location and direction, was used as reference. If necessary, the catheter was steam-shaped according to the information of CT to facilitate accurate catheterization and drawing back of blood.

Simultaneous right and left adreal venous sampling before and 15 minutes after injection of 0.25mg adrenocorticotropic hormone (ACTH) were performed.

2. Interpretation of angiography

The craniocaudal level of the RAV orifice was specified relative to vertebral bodies and the direction of the RAV at the branching portion from the IVC by

venography which was performed during adrenal venous sampling. The position of the RAV orifice compared to the horizontal position of the IVC was also evaluated. Furthermore, we examined whether a common trunk for the RAV and accessory hepatic or other veins was formed before entering the IVC. The result of angiographic evaluation of the right adrenal vein was compared with CT diagnosis.

Three dimensional image of the adrenal vein

Three dimensional image including

Results

Interpretation of CT.

1. Degree of visualization of the RAV

The RAV was detected in 42 (100%) of 42 patients according to our identification criteria (Fig. 2).

2. Relationship of the RAV to an accessory hepatic vein

The RAV and an accessory hepatic vein formed a common trunk before entering the IVC in 3 patients (7.1%). In 13 patients, the RAV orifice was located within 2mm from that of the accessory hepatic vein (31.0% of the 42 patients).

3. Location of the RAV orifice in relation to surrounding structures

The orifice was craniocaudally located between the level of T10 and L1 (Fig. 3). In 39 (92.9%) of the 42 patients, the RAV joined the IVC at the level ranging from the middle third of T11 to the lower third of T12. Angle representing the position of the orifice along the circumference of the IVC ranged from 5° to 52° (mean, 31°). The RAV joined the IVC in the right posterior quadrant in 100%.

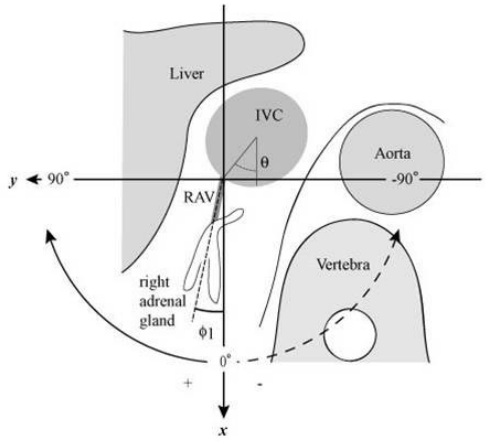

Fig. 2. The position of the orifice of the right adrenal vein is evaluated along the circumference of the IVC as an angle in the *x–y* plane. The angle (X1) between the RAV and *x*-axis when the RAV was projected onto the *x–y* plane is also measured.

4. Direction of the RAV at the branching portion from the IVC

The direction of the RAV from the IVC was posterior and rightward in 33 (78.6%) and posterior and leftward in 9 (21.4%) of the 42 patients. The angle(X1) ranged from -53° to 45° (mean, 7.7°).

The angle(X2) ranged from 0 to 153° (mean, 69.9°), and most patients showed a value between 50° and 90°. The direction of the RAV from the IVC was caudal in 33 (78.6%) and cranial in 9 (21.4%) of the 42 patients.

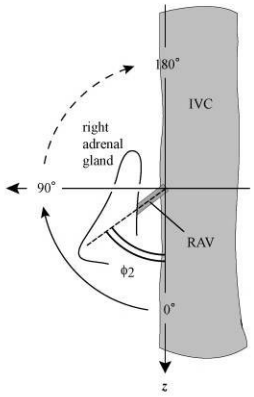

Fig. 3. The craniocaudal angle of the right adrenal vein with z-axis in the vertical plane. IVC = inferior nena cava.

Interpretation of angiography.

In all the patients, craniocaudal level of the RAV orifice coincided with that diagnosed by MDCT in 27 of 42 patients. In the remaining 15 patients, the difference of the vertebral level between CT and angiographic diagnosis is 1/3 vertebral height in 13 patients and 2/3 vertebral height in 2 patients.

Success rate of selective adrenal venous sampling was 100%.

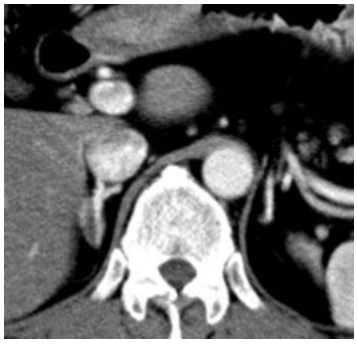

Fig. 4. The most frequent anatomy of the RAV which runs medially to enter into right posterior quadrant of the IVC.

Fig. 5. The RAV runs laterally to enter into IVC.

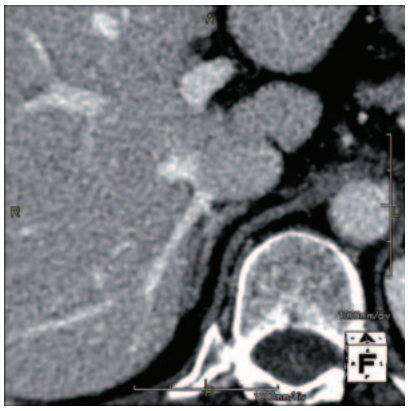

Fig. 6. The RAV-accessory hepatic vein common trunk. The right adrenal vein joins with the accessory hepatic vein to make common trunk.

Discussion

MDCT enabled the identification of the RAV in all the patients. The enhanced structure of the RAV was detectable using 64-slice MDCT. The RAV anatomy including the position in relation to the IVC and surrounding structures was well evaluated. The right adrenal venous anatomy diagnosed by MDCT coincided well with angiographic findings.

The difficulty associated with RAV catheterization appears to result from the pre-angiographic unpredictability of the variable anatomy of the RAV, which is a small vein that usually drains directly into the IVC at a variable angle. In the most typical anatomy in our series, RAV runs medially to enter into posterior lateral aspect of the IVC. In this type, RAV could be catheterized using original shape of the right adrenal venous catheter. Pre-angiographic information about the level relative to vertebral bodies and discs helps catheterization, reducing the total time of procedure. As to the transverse direction of the RAV, in 21.4% of the patients, RAV has posterior leftward direction. In this type re-shaping of the tip of the RAV catheter is sometimes required to make the tip of the catheter parallel to the RAV for good blood drawing. Catheterization into right adrenal vein which has common trunk with accessory hepatic vein is more difficult because of the complicated route to the right adrenal vein. However, pre-angiographic information of this anatomy helps catheter manipulation and adequate steam-shaping of the catheter enabling successful venous sampling.

Recently, adrenal venous sampling is regarded as the only reliable method in diagnosing laterality of aldosterone hypersecretion [2-6]. Patients with unilateral aodosterone hypersecretion can be successfully treated by lapaloscopic adrenarectomy, while patients with bilateral hypersecretion are treated medically. Therefore, pre-angiographic visualization of fine adrenal vein is essential in the successful management of patients with primary aldosteronism.

In conclusion, MDCT enabled the identification of the RAV and delineation of its anatomy, including the position and relationship to the surrounding structures such as the IVC in a high percentage of patients. This preoperative information helps accurate catheterization of the RAV for adrenal venous sampling.

Visualization of the artery of Adamkiewicz

Abstract

Accurate localization of the artery of Adamkiewicz (AKA) is important in planning treatment of patients with thoracoabdominal aortic disease. We assessed the usefulness of three-dimensional imaging devices such as multi-detector-row helical computed tomography (MDCT) and 3 Tesla (T) MRI in the preoperative evaluation of the artery of Adamkiewicz (AKA) and its parent artery. Patients with thoracoabdominal vascular diseases underwent MDCT of the entire aorta and iliac arteries. Sub-millimeter collimation was used with the rapid injection of concentrated contrast material. The AKA and intercostal/lumbar arteries from which it originated were examined using multiplanar and curved planar reconstruction images and cine-mode display. The visualization of the AKA, as well as its branching level and site of origin, and the continuity of the intercostal/lumbar arteries with the AKA were investigated. 3T-MRA was also performed in patients whose AKA was difficult to visualize because of artifact from bony structures.

In 90% of the patients the AKA was clearly visualized. The entire length from the trunk of the intercostal/lumbar arteries to the AKA, and finally to the anterior spinal artery could be traced using cine-mode display or on curved planar reconstruction images in 80%. These patients were treated by open surgical treatment based on a consideration of the vascular supply to the AKA or treated by stentgraft insertion. No postoperative ischemic spinal complications occurred in these patients except two. 3T-MRA increases success rate of visualizing AKA

when used with MDCT. MDCT with Sub-millimeter collimation and a rapid injection protocol permits the evaluation of the AKA for its entire length and provides information on the intercostal and lumbar arteries and entire aorta. 3T-MRA has complementally role with MDCT.

Introduction

Accurate localization of the artery of Adamkiewicz (AKA) is important in planning the surgical or interventional radiological treatment of patients with thoracoabdominal aortic disease. Preoperative information on the localization of this artery may reduce the risk of postoperative ischemic spinal complications [10-16]. Although conventional angiography is reported to be useful [12-15], various complications of spinal angiography have been described [12,14]. Noninvasive detection of the AKA using magnetic resonance imaging (MRI) and its usefulness for surgery has also been reported with a detectability of 69 to 84% [16-18]. Due to the limited scanning field of view, however, MRI cannot demonstrate the entire aorta and intercostal and lumber arteries simultaneously with information on the AKA. Multi-detector-row helical CT (MDCT) with a four-slice detector and 2-mm collimation has recently been reported to be effective in demonstrating the AKA [19], although that study did not focus on patients requiring an aortic vascular graft or stentgraft in the T8–T12 region, where the AKA likely originates and postoperative ischemic spinal complications are likely to occur. Moreover, no previous studies have included a radiological evaluation of the patency of the parent intercostal or lumbar arteries branches of the AKA, or the intercostal/lumbar arteries adjacent to the parent artery, which can provide collaterals to the AKA when needed.

Recently, MDCT with 8, 16, 32, or 64 detector rows has become available, permitting imaging of the entire aorta and iliac arteries with less than 1-mm collimation. This study evaluated the capacity of 16-slice MDCT with 0.5-mm collimation and a rapid injection protocol to evaluate the continuity of the AKA and its parent artery and to visualize the intercostals and lumbar arteries adjacent to the parent artery for preoperative evaluation of patients with thoracoabdominal aortic disease.

Materials and Methods

Patients

We performed a retrospective analysis of CT images from 36 consecutive patients (32 men, 4 women; mean age, 56.1 years; range, 34-77 years) with diagnosis of thoracic aortic aneurysm (14 patients) or aortic dissection (22 patients) including thoracoabdominal aorta, who underwent aortic replacement surgery (25 patients) or stentgraft insertion (11 patients). Informed consent for contrast-enhanced CT had been obtained from all patients before the examinations.

Radiological Imaging

The CT scanner was an Aquilion 16-detector row helical CT scanner (Toshiba, Tokyo, Japan). Scans were obtained with the following parameters: 0.5 second per rotation, 0.5 mm collimation. Patients were requested to hold their breath for approximately 20 seconds during the scanning followed by shallow breathing.

Before scanning was started, 130-150 ml of contrast material (Iopamiron, Schering, Berlin, Germany; 370 mgI/ml) was injected via an antecubital vein at a rate of 4.0-4.5 ml/s. If a suitable antecubital vein could not be found, the right external jugular vein was used for contrast injection. The scan delay was set using an automatic triggering system (SureStart, Toshiba Medical Systems). Continuous low-dose CT fluoroscopy (120 kV, 50 mA) at the level of the ascending aorta was initiated 10 s after the start of contrast injection. The CT value in a circular region of interest placed in the ascending aorta was measured 3 times per second, and when the CT value reached the threshold (absolute CT value of 85 Hounsfield Units) at 3 consecutive sampling points, helical scanning was started automatically.

Axial slices were reconstructed with a 0.5-mm slice thickness at 0.3-mm intervals. For the evaluation of the artery of Adamkiewicz, the reconstruction field of view was set to the area around the aorta and spine.

Images were processed using a stand-alone workstation (Zio M900 Quadra, Amin, Tokyo, Japan). Volume-rendering images of the entire aorta were routinely generated. Curved planar reconstruction (CPR) images were generated so that the anterior spinal artery, the artery of Adamkiewicz, and its parent artery could be traced over as long a distance as possible. 3T-MRA was also performed in patients whose AKA was difficult to visualize because of artifact from bony structures.

The following points were evaluated: 1. the side and level of the artery of Adamkiewicz; 2. the continuity of the artery of Adamkiewicz with the anterior spinal artery, the intercostal/lumbar arteries, and their posterior branches; 3. the patency of the intercostal/lumbar arteries branching from the artery of Adamkiewicz.

Results

In 33 of the 36 patients (91.7%), the artery of Adamkiewicz within the bony spinal canal was clearly delineated, permitting both the level of origin and the side of the artery to be identified (Fig. 7). In 3 patients with a thoracic aortic aneurysm, the artery of

Adamkiewicz was not visualized and enhancement of the anterior spinal artery was poor. The continuity over the entire length from the stem of the intercostal/lumbar arteries and their posterior branches, to the artery of Adamkiewicz, and finally to the anterior spinal artery could be traced in 29 of the 36 (80.1%) patients (Fig. 7). In two of the remaining 7 patients, the continuity was visualized by MRI (Fig. 8). In the remaining patient, continuity between the posterior branch of the intercostal / lumbar artery and the artery of Adamkiewicz could not be clearly visualized. In 13 patients the parent artery of AKA was occluded (Fig. 9).

In 25 patients who underwent aortic replacement surgery, intercostal arteries were reconstructed based on the information of CT localization of the artery of Adamkiewicz. Two patients with aortic dissection showed incomplete spinal complication.

Although the origin of AKA was completely coverd by stentgraft in 8 of the the 11 patients who underwent stentgraft insertion, no spinal complication was dedtected in the stent group. In these 8 patients, AKA was visualized by follow up CT after stentgraft insertion.(Fig. 10)

Fig. 7. Three dimensional reconstruction of the artery of Adamkiewicz visualized by MDCT image. Curved planar image along the intercostal artery through anterior spinal artery clearly demonstrates the origin and anatomy of the artery of Adamkiewicz.
The patency of the artery of Adamkiewicz from its origin through the anterior spinal artery can be diagnosed.

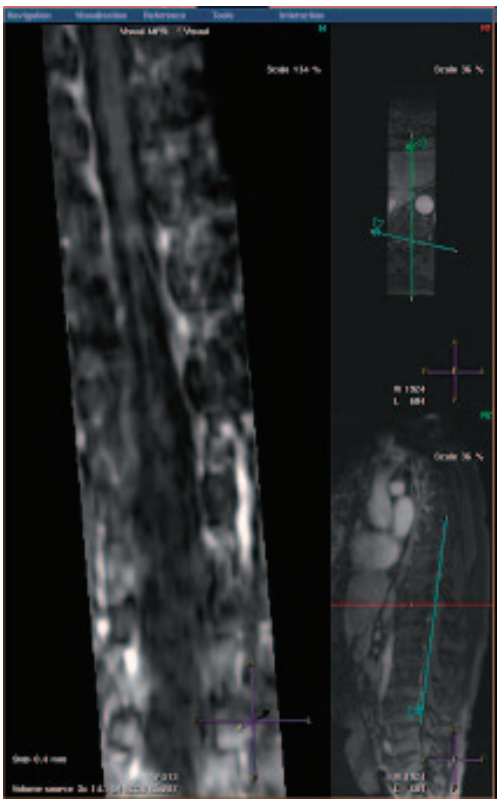

Fig. 8. MRI image using Keyhole technique demonstrates the artery of Adamkiewicz and the anterior spinal artery. Because of the high temporal resolution, the artery of Adamkiewicz can be distinguished from the radiculomedullary vein.

Fig. 9. Curved planar image along the intercostal artery through anterior spinal artery shows the intercostal artery, its posterior branch, the artery of Adamkiewicz and the anterior spinal artery. The origin of the intercostal artery is occluded due to thick mural thrombus of thoracoabdominal aortic aneurysm.

(a) (b)

Fig. 10. MDCT after stentgraft insertion to thoracic aorta. (a): Stent graft can be seen from the aortic arch through the thoracoabdominal aorta by volume rendering image. (b): Curved planar reformation image shows the intercostal artery, its posterior branch, the artery of Adamkiewicz, and the anterior spinal artery. Although the origin of the intercostal artery is covered with the stentgraft, the blood flow to the spine is maintained by collateral circulation to these arteries.

Discussion

Sixteen-slice MD-CT with 0.5-mm collimation and a rapid injection protocol permitted the artery of Adamkiewicz to be visualized and also provided information concerning the adjacent intercostal/lumbar arteries. The continuity from the intercostal/lumbar arteries through the artery of Adamkiewicz could be traced in high percentage of the patients. Patients with aortic diseases involving the thoracoabdominal region typically present with stenosis or occlusion of the intercostal/lumbar arteries, and the parent arteries of the artery of Adamkiewicz (i.e., the intercostal/lumbar arteries) must therefore also be evaluated. Some patients were found to have occlusion of the intercostal/lumbar arteries at multiple levels in the region superior or inferior to the origin of the artery of Adamkiewicz. In the patients in the present study, the vascular supply to the artery of Adamkiewicz was thought to be highly dependent on collaterals. Concerning the patients who underwent stentgraft insertion, no patients had spinal complication after the procedure. Vascular supply to the spinal cord in these patients were thought to be maintained by collateral circulation.

Although MDCT permits visualization of AKA, continuity from the stem of the intercostal/lumbar arteries and their posterior branches, to the artery of AKA is sometimes difficult because of close approximation of the artery and the spine. In such cases, MRI plays an complementary role of MDCT.

Recently developed 3T-MRI will enable visualization of AKA with high temporal resolution permitting distinction between AKA and radiculomedullary vein. (Fig. 8) In conclusion, MDCT with Sub-millimeter collimation and a rapid injection protocol permits the evaluation of the AKA for its entire length and provides information on the intercostal and lumbar arteries and entire aorta, which provides useful information for treatment of thoracoabdominal aortic diseases.

Reference

[1] Mulatero P, Stowasser M, and Loh KC. Increased diagnosis of primary aldosteronism, including surgically correctable forms, in centers from five continents. *J Clin Endocrinol Metab* **89**, 1045-1050, 2004.

[2] Magill SB, Raff H, Shaker JL, and et al. Comparison of adrenal vein sampling and computed tomography in the differentiation of primary aldosteronism. *J Clin Endocrinol Metab* **86**, 1066-1071, 2001.

[3] Espiner EA, Ross DG, Yandle TG, Richards AM, and Hunt PJ. Predicting surgically remedial primary aldosteronism: role of adrenal scanning, posture testing, and adrenal vein sampling. *J Clin Endocrinol Metab* **88**, 3637-3644, 2003.

[4] Rossi GP, Bernini G, and Caliumi C. A prospective study of the prevalence of primary aldosteronism in 1,125 hypertensive patients. *J Am Coll Cardiol* **48**, 2293-2300, 2006.

[5] Young WF, Stanson AW, Thompson GB, Grant CS, Farley DR, and van Heerden JA. Role for adrenal venous sampling in primary aldosteronism. *Surgery* **136**, 1227-1235, 2004.

[6] Satoh F, Abe T, Tanemoto M, et al. Localization of aldosterone-producing adrenocortical adenomas: significance of adrenal venous sampling. *Hypertens Res* **30**, 1083-1095, 2007.

[7] Fogari R, Preti P, Zoppi A, Rinaldi A, Fogari E, and Mugellini A. Prevalence of primary aldosteronism among unselected hypertensive patients: a prospective study based on the use of an aldosterone/renin ratio above 25 as a screening test. *Hypertens Res* **30**, 111-117, 2007.

[8] Plouin PF, Amar L, and Chatellier G. Trends in the prevalence of primary aldosteronism, aldosterone-producing adenomas, and surgically correctable aldosterone-dependent hypertension. *Nephrol Dial Transplant* **19**, 2418-2419, 2004.

[9] Matsuura T, Takase K, et al. Radiological Anatomy of the right adrenal vein: Preliminary experience with multidetector-row computed tomography. *AJR* **191**, 401-408, 2008.

[10]Svenson LG and Crawford ES. *Cardiovascular and vascular disease of the aorta.* WB Saunders,

Philadelphia, 1997.
[11]Svenson LG, Crawford ES, Hess KR, Cosseli JS, and Safi HJ. Experience with 1509 patients undergoing thoracoabdominal aortic operations. *J Vasc Surg* **17**, 357-370, 1993.
[12]Williams GM, Perler BA, Burdick JF, et al. Angiographic localization of spinal cord blood supply and its relationship to postoperative paraplegia. *J Vasc Surg* **13**, 23-33, 1991.
[13]Fereshetian A, Kadir S, Kaufman SL, et al. Digital subtraction angiography in patients undergoing thoracic aneurysm surgery. *Cardiovasc Intervent Radiol* **12**, 7-9, 1989.
[14]Savader SJ, Williams GM, Trerotola SO, et al. Preoperative spinal artery localization and its relationship to postoperative neurologic complications. *Radiology* **189**, 165-171, 1993.
[15]Heinemann MK, Brassel F, Herzog T, Dresler C, Becker H, and Borst HG. The role of spinal angiography in operations on the thoracic aorta: myth or reality? *Ann Thorac Surg* **65**, 346-351, 1998.
[16]Hyodoh H, Kawaharada N, Akiba H, Tamakawa M, Hyodoh K, Fukada J, Morishita K, and Hareyama M. Usefulness of preoperative detection of artery of Adamkiewicz with dynamic contrast-enhanced MR. *Angiogr Radiol* **236**, 1004-1009, 2005.
[17]Yoshioka K, Niinuma H, Ohira A, et al. MR angiography and CT angiography of AKA: noninvasive preoperative assessment of thoracoabdominal aortic aneurysm. *RadioGraphics* **23**, 1215-1225, 2003.
[18]Yamada N, Okita Y, Minatoya K, et al. Preoperative demonstration of the Adamkiewicz artery by magnetic resonance angiography in patients with descending or thoracoabdominal aortic aneurysms. *Eur J Cardiothorac Surg* **18**, 104-111, 2000.